Journal of Biomechanics 94 (2019) 165–169

Contents lists available at ScienceDirect

Journal of Biomechanics

journal homepage: www.elsevier.com/locate/jbiomech
www.JBiomech.com

Biomechanical model of swimming rehabilitation after hip and knee surgery

Zoran Gojkovic [a], Tijana Ivancevic [b], Bojan Jovanovic [c]

[a] University of Novi Sad, Faculty of Medicine, Clinical Centre of Vojvodina, Clinic for Orthopedic Surgery and Traumatology, Novi Sad, Serbia
[b] Tesla Science Evolution Institute, Australia
[c] Sports Academy, Belgrade, Serbia

ARTICLE INFO

Article history:
Accepted 27 July 2019

Keywords:
Hip and knee rehabilitation
Legs propulsion in swimming
Kirchhoff-Lagrangian dynamics
Numerical simulation

ABSTRACT

As a low-to-moderate intensity rehabilitation exercise after hip and knee surgery, we propose a dynamical model of the legs motion through the water medium in freestyle and backstroke swimming. We formulate a general Kirchhoff-Lagrangian dynamics model of the legs-propulsion through the water in post-surgical rehabilitation swimming.

We start by defining the two-leg-propulsion configuration manifold. This is composed of eight Euclidean groups of rigid motions in 3D space for each of the four leg segments. Next, we define Newton-Euler dynamics for each segment. This single segmental dynamics is further generalized into Lagrangian dynamics for the whole leg-propulsion system. Finally, the water effects are added in the form of Kirchhoff's vector cross-products.

In agreement with orthopaedic recommendations for post-surgical rehabilitation, numerical simulation is performed on a simplified version of the full Kirchhoff-Lagrangian dynamics model, which we call the "robotic swimming leg" – with intentionally reduced number of (microscopic, non-sagittal) degrees-of-freedom.

The purpose of this development is both qualitative, for medical and physiotherapist practitioners to study, and quantitative, for biomechanics experts to analyze and further develop.

1. Introduction

Biomechanical modeling is becoming more and more important for the successful outcome of the hip-replacement and/or knee-reconstruction surgery (Assassi and Magnenat-Thalmann, 2014; O'Connor et al., 1999; Ardestani et al., 2019; Gojkovic and Ivancevic, 2016; Gojkovic et al., 2017; Ivancevic et al., 2019), as well as for new material and implant research and innovation (see Yahia, 2015; Gojkovic, 2015).

Patient-reported outcomes confirm that joint replacement is an effective treatment for disabling hip and/or knee joint diseases (Rolfson et al., 2016). Recent survey of the health-related quality of life after a large number of joint replacements (Konopka et al., 2018) shows that primary hip and knee replacement surgery mostly result in increased patient quality of life, which is somewhat lower (but still positive) in cases of the secondary (revision) surgery, with large variations in individual patients.

The ultimate objective of the knee and/or hip replacement/reconstruction surgery, followed by appropriate rehabilitation exercises to maintain the necessary strength and coordination of both extensor and flexor muscles, is to provide the injured knee and/or hip with the normal function (see Yahia, 1997; Duval and St-Onge, 1997; Sjolander and Johansson, 1997; St-Onge et al., 2004; Gallo et al., 2012 and the references therein).

In case of the hip joint rehabilitation, the particular emphasis must be given to the *iliopsoas* muscle, since its passive and/or active insufficiency inevitably causes pathological anomalies of both static and dynamic nature (see Michele, 1962; Ivancevic et al., 2017).

In recent years, bicycle riding (or, more generally, cyclic, full-leg, bipedal) rehabilitation exercises after hip and knee surgery have been proposed in Gojkovic and Ivancevic (2016), Gojkovic et al. (2017).

Alternatively, the *aquatic therapy* in the rehabilitation of leg injuries has been used for several decades (see Prins and Cutner, 1999 and the references therein). When performed in the full-size swimming pool, all swimming techniques can be used, provided they are performed in a fully controlled fashion.

The complexity of the full-body swimming dynamics is too high for rigorous modeling, due to different arm motions (see, e.g.

E-mail address: Zoran.Gojkovic@mf.uns.ac.rs (Z. Gojkovic)

https://doi.org/10.1016/j.jbiomech.2019.07.035
0021-9290/

Gourgoulis et al., 2008) including many *degrees-of-freedom* (DOFs) with fine muscular coordination (Vaz et al., 2016) in four different ways, with longer or shorter underwater swimming (Veiga et al., 2016), as well as inevitably involved fluid dynamics (see Zaidi et al., 2008; Takagi et al., 2016 and the references therein). Much simpler problem is to model swimming propulsion by legs only, even if fluid dynamics is properly included.

In the present paper, as a recommended rehabilitation exercise after hip and knee surgery, we model legs motion/propulsion in freestyle and backstroke swimming, using the Kirchhoff-Lagrangian equations of motion through water medium.

2. The model

Swimming propulsion, in all four techniques, involves the following leg segments:

1. Upper leg (thigh, supported by Femur),
2. Lower leg (shank, supported by Tibia and Fibula),
3. Proximal foot (foot, supported by Tarsals and Metatarsals), and
4. Distal foot (toes, supported by Phalanges)

– all influenced by viscoelastic properties of the leg *fascia* (see Yahia et al., 1992, 1993).

These leg segments are connected by human joints which are much more flexible that robot joints (see Ivancevic and Ivancevic, 2008 and the references therein). This fact is even more prominent in elite swimmers: besides hinge-like macroscopic rotations, all leg joints of swimmers also include microscopic translations in all three Cartesian directions. Based on this fact, we propose a general Kirchhoff-Lagrangian dynamics model in which the above leg segments are mechanically represented as flexibly-coupled Ivancevic, 2009 Newtonian rigid bodies moving through water in 3D space (see Ivancevic and Ivancevic, 2006; Ivancevic and Ivancevic, 2006). Formally, each leg segment represents a 6-parameter Euclidean Lie group $SE(3)$ of rigid motions in 3D space $\mathbb{R}^3$, defined as a Cartesian product[1] of the 3D rotation group $SO(3)$ and 3D translation group $\mathbb{R}^3 : SE(3) := SO(3) \times \mathbb{R}^3$ (see Ivancevic and Ivancevic, 2012 and the references therein).

Geometrically, as each leg has four $SE(3)$-segments: {thigh, shank, foot, toes}, we are dealing with the 48-dimensional Riemannian configuration manifold (Ivancevic and Ivancevic, 2006; Ivancevic, 2010b):

$M^{48}_{\rm swim} = M^{24}_{\rm left} \times M^{24}_{\rm right}$ with two connected components (left leg $M^{24}_{\rm left}$ and right leg $M^{24}_{\rm right}$) working together to propel the body through the water. This legs-swimming configuration manifold is formally defined as:

$$M^{48}_{\rm swim} = \left\{ \begin{array}{c} M^{24}_{\rm left} \equiv SE(3)^{\rm thigh}_{\rm left} \times SE(3)^{\rm shank}_{\rm left} \times SE(3)^{\rm foot}_{\rm left} \times SE(3)^{\rm toes}_{\rm left} \\ M^{24}_{\rm right} \equiv SE(3)^{\rm thigh}_{\rm right} \times SE(3)^{\rm shank}_{\rm right} \times SE(3)^{\rm foot}_{\rm right} \times SE(3)^{\rm toes}_{\rm right} \end{array} \right\} \Longrightarrow \boxed{\rm propulsion}.$$

On the configuration manifold $M^{48}_{\rm swim}$ we will develop the general Kirchhoff-Lagrangian dynamics in the following subsections.

[1] More rigorously, instead of the commutative Cartesian product, we should use the noncommutative product; however, this would lead to noncommutative geometry and algebra, which is a non-necessary complication in the current context.

2.1. Newton-Euler dynamics of a single leg segment

For each leg segment (thigh, shank, foot, or toes), the vector Newton-Euler $SE(3)$-dynamics are given in standard Cartesian (x, y, z)-coordinates as:

$$\begin{aligned} \dot{\boldsymbol{p}} &:= \boldsymbol{M}_{\rm seg}\dot{\boldsymbol{v}} = \boldsymbol{F}_{\rm seg} + \boldsymbol{p} \times \boldsymbol{\omega}, \\ \dot{\boldsymbol{\pi}} &:= \boldsymbol{I}_{\rm seg}\dot{\boldsymbol{\omega}} = \boldsymbol{T}_{\rm seg} + \pi \times \omega + \boldsymbol{p} \times \boldsymbol{v}, \end{aligned} \tag{1}$$

where overdot denotes time derivative, while the leg segments' inertial distribution is given by the following diagonal mass and inertia matrices:

$$\boldsymbol{M}_{\rm seg} = {\rm diag}\{m_x, m_y, m_z\} \qquad \text{and} \qquad \boldsymbol{I}_{\rm seg} = {\rm diag}\{I_x, I_y, I_z\},$$

where the principal moments of inertia $\boldsymbol{I}$ are defined by volume integrals:

$$I_x = \int_{\mathbb{R}^3} \rho(z^2 + y^2)dxdydz, \; I_y = \int_{\mathbb{R}^3} \rho(x^2 + y^2)dxdydz,$$
$$I_z = \int_{\mathbb{R}^3} \rho(x^2 + y^2)dxdydz,$$

which depend on each leg segment's average 3D density function $\rho = \rho(x, y, z)$.

Each leg segments' linear and angular velocity vector fields are given respectively by:

$$\begin{aligned} \boldsymbol{v} &= \dot{\boldsymbol{x}} = [v_x, v_y, v_z]^T = [\dot{x}, \dot{y}, \dot{z}]^T, \\ \boldsymbol{\omega} &= \dot{\boldsymbol{\varphi}} = [\omega_x, \omega_y, \omega_z]^T = [\dot{\varphi}_x, \dot{\varphi}_y, \dot{\varphi}_z]^T, \end{aligned}$$

where $\boldsymbol{x} := [x, y, z]^T$ are Cartesian coordinates of the leg segments' center-of mass (CoM) and $\boldsymbol{\varphi} = [\varphi_x, \varphi_y, \varphi_z]^T = [\varphi_{\rm roll}, \varphi_{\rm pitch}, \varphi_{\rm yaw}]^T$ are its Euler angles (roll, pitch and yaw). The co-vector fields, including muscular, gravitational and other external forces and torques acting on the leg segment are:

$$\boldsymbol{F}_{\rm seg} = [F_x, F_y, F_z] \qquad \text{and} \qquad \boldsymbol{T}_{\rm seg} = [T_x, T_y, T_z],$$

while the corresponding linear and angular momentum co-vector fields are:

$$\begin{aligned} \boldsymbol{p} &= \boldsymbol{M}_{\rm seg}\boldsymbol{v} = [p_x, p_y, p_z] = [m_x v_x, m_y v_y, m_z v_z], \qquad (\text{such that } \boldsymbol{F}_{\rm seg} = \dot{\boldsymbol{p}}) \\ \boldsymbol{\pi} &= \boldsymbol{I}_{\rm seg}\boldsymbol{\omega} = [\pi_x, \pi_y, \pi_z] = [I_x\omega_x, I_y\omega_y, I_z\omega_z], \qquad (\text{such that } \boldsymbol{T}_{\rm seg} = \dot{\boldsymbol{\pi}}). \end{aligned}$$

For the legs-propulsion in swimming, the most important thing is that the muscular (driving) parts of forces and torques are periodic with optimal amplitudes and frequencies.

2.2. Lagrangian dynamics for the whole leg motion

Next, we need to generalize the above single-segment Newton-Euler dynamics to the four-segment equations of motion for the whole leg in swimming. For simplicity of the vector-matrix notation, we use the same symbols as above, but from now on they refer to the four-segment leg, including:

$$\begin{aligned} \boldsymbol{M} &= \boldsymbol{M}_{\rm leg} = \boldsymbol{M}_{\rm thigh} + \boldsymbol{M}_{\rm shank} + \boldsymbol{M}_{\rm foot} + \boldsymbol{M}_{\rm toes}, \\ \boldsymbol{I} &= \boldsymbol{I}_{\rm leg} = \boldsymbol{I}_{\rm thigh} + \boldsymbol{I}_{\rm shank} + \boldsymbol{I}_{\rm foot} + \boldsymbol{I}_{\rm toes}, \\ \boldsymbol{F} &= \boldsymbol{F}_{\rm leg} = \boldsymbol{F}_{\rm thigh} + \boldsymbol{F}_{\rm shank} + \boldsymbol{F}_{\rm foot} + \boldsymbol{F}_{\rm toes}, \\ \boldsymbol{T} &= \boldsymbol{T}_{\rm leg} = \boldsymbol{T}_{\rm thigh} + \boldsymbol{T}_{\rm shank} + \boldsymbol{T}_{\rm foot} + \boldsymbol{T}_{\rm toes}. \end{aligned}$$

Lagrangian dynamics can be formulated in the following way (see, e.g. Ivancevic, 2010a and the references therein). The whole-leg generalization of Eqs. (1) can be derived from the following Lagrangian (kinetic) energy function:

$$L(v,\boldsymbol{\omega}) = E_{\text{kin}}(v) + E_{\text{kin}}(\boldsymbol{\omega}) = \frac{1}{2}\boldsymbol{v}^T\boldsymbol{M}\boldsymbol{v} + \frac{1}{2}\boldsymbol{\omega}^T\boldsymbol{I}\omega, \tag{2}$$

including both translational kinetic energy: $E_{\text{kin}}(v) = \frac{1}{2}\boldsymbol{v}^T\boldsymbol{M}\boldsymbol{v}$ and rotational kinetic energy: $E_{\text{kin}}(\boldsymbol{\omega}) = \frac{1}{2}\boldsymbol{\omega}^T\boldsymbol{I}\omega$.

As usual (using the index notation for partial derivatives: $L_z = \frac{\partial L}{\partial z}$), we start by deriving the dissipation-free and force-free, conservative Lagrangian equations of both translational and rotational motion of all leg segments:

$$\dot{L}_{\boldsymbol{v}} = L_{\boldsymbol{x}} \qquad \text{and} \qquad \dot{L}_{\boldsymbol{\omega}} = L_{\boldsymbol{\varphi}}. \tag{3}$$

Next, we extend the conservative Lagrangian dynamics (3) by including the ever-present friction forces and torques (derived from the Rayleigh dissipative function), as well as both internal-muscular and external forces and torques, including gradient forces E_{v^i} and torques E_{ω^i} derived from the leg potential energy $E_{\text{pot}}(x,\varphi) = E_{\text{pot}}(x) + E_{\text{pot}}(\varphi)$. In such a way, we obtain the dissipative and forced Lagrangian dynamics for the leg translations and rotations during swimming propulsion:

$$\dot{L}_{\boldsymbol{v}} + R_{\boldsymbol{v}} = L_{\boldsymbol{x}} + \boldsymbol{F} \qquad \text{and} \qquad \dot{L}_{\boldsymbol{\omega}} + R_{\boldsymbol{\omega}} = L_{\boldsymbol{\varphi}} + \boldsymbol{T}, \tag{4}$$

where $R_{\boldsymbol{v}}$ and $R_{\boldsymbol{\omega}}$ are gradients of the translational and rotational Rayleigh dissipative functions, $R(x, v)$ and $R(\varphi, \boldsymbol{\omega})$, respectively. Provided the muscular (driving) parts of forces $\boldsymbol{F}$ and torques $\boldsymbol{T}$ are periodic with optimal amplitudes and frequencies, Eqs. (4) would represent a proper leg-propulsion dynamics in the absence of a water environment.

2.3. Kirchhoff–Lagrangian dynamics model for the whole leg propulsion through water in swimming

As the swimmer's legs are immersed in water, Eqs. (4) need to be further extended by adding several mixed rotational-translational cross-products to represent water influences (coming from fluid dynamics). In this way, we obtain the following *Kirchhoff–Lagrangian equations* (see, e.g. Lamb, 1932; Leonard, 1997, or the original work of Kirchhoff in German):

$$\begin{aligned} \dot{L}_{\boldsymbol{v}} + R_{\boldsymbol{v}} &= L_{\boldsymbol{x}} + \boldsymbol{F} + L_{\boldsymbol{v}} \times \boldsymbol{\omega}, \\ \dot{L}_{\boldsymbol{\omega}} + R_{\boldsymbol{\omega}} &= L_{\boldsymbol{\varphi}} + \boldsymbol{T} + L_{\boldsymbol{\omega}} \times \boldsymbol{\omega} + L_{\boldsymbol{v}} \times \boldsymbol{v}, \end{aligned} \tag{5}$$

with forces and torques now split into muscular parts and external parts:

$$\boldsymbol{F} = \boldsymbol{F}_{\text{musc}} + \boldsymbol{F}_{\text{extern}} \qquad \text{and} \qquad \boldsymbol{T} = \boldsymbol{T}_{\text{musc}} + \boldsymbol{T}_{\text{extern}}, \tag{6}$$

such that the muscular parts are periodic:

$$\begin{aligned} \boldsymbol{F}_{\text{musc}} &= A_{\text{tr}} \cos(\phi_{\text{tr}} t - \tau_{\text{tr}}) \qquad \text{and} \\ \boldsymbol{T}_{\text{musc}} &= A_{\text{rot}} \cos(\phi_{\text{rot}} t - \tau_{\text{rot}}), \end{aligned} \tag{7}$$

with amplitudes (A_{tr}, A_{rot}), frequencies (ϕ_{tr}, ϕ_{rot}) and time-delays (τ_{tr}, τ_{rot}) optimized for the particular swimming technique.

Finally, for computational purposes (so that for-loops upon all leg segments can be used) as well as for the clarification of the segmental labeling, we convert the vector Kirchhoff–Lagrangian Eqs. (5) into the follow index form:

$$\dot{L}_{v^i} + R_{v^i} = L_{x^i} + F_i + \varepsilon^j_{ik} L_{v^j} \omega^k, \qquad (i,j,k = 1,\ldots,4) \tag{8}$$

$$\dot{L}_{\omega^i} + R_{\omega^i} = L_{\varphi^i} + T_i + \varepsilon^j_{ik} L_{\omega^j} \omega^k + \varepsilon^j_{ik} L_{v^j} v^k, \tag{9}$$

where ε^j_{ik} is the Levi-Civita permutation symbol and Einstein's summation convention over repeated indices is used. The tensor Kirchhoff–Lagrangian Eqs. 8,9 represent our general dynamics model for the following leg segments in swimming propulsion:

$i,j,k = 1$: Upper leg, actuated mainly by Iliopsoas (hip flexor) and Gluteus Maximus (hip extensor);
$i,j,k = 2$: Lower leg, actuated mainly by Quadriceps Femoris (knee extensor) and Hamstrings (knee flexor);
$i,j,k = 3$: Proximal foot, actuated mainly by proximal tendons of Soleus (plantar flexor) and Tibialis Anterior (dorsal flexor),
$i,j,k = 4$: Distal foot, actuated by distal tendons of Soleus (phalangeal flexor) and Tibialis Anterior (phalangeal extensor).

Tensor Eqs. 8,9 represent our final model for the leg-propulsion dynamics in general swimming (all four techniques), provided the muscular parts (6) of the forces $\boldsymbol{F} = F_i$ and torques $\boldsymbol{T} = T_i$ (for $i = 1,\ldots,4$) are periodic with optimal amplitudes and frequencies (7) for each particular swimming technique.

3. Simulations: "Robotic Leg motion in freestyle and backstroke swimming

In agreement with standard orthopaedic recommendations for post-surgical rehabilitation, the legs motion must be restricted to the *sagittal plane* only. By applying this restriction we obtain the so-called "robotic leg" – with intentionally eliminated microscopic degrees-of-freedom. Numerical simulation is performed on this simplified version of the general tensor Kirchhoff–Lagrangian Eqs. 8,9. For this simplified simulation, we apply the usual assumption that the above leg segments are interconnected with hinge-type joints (only) with fixed constrained amplitudes, thus restricting the whole leg motion to the sagittal plane.

The following simplifications are made for the simulated "robotic swimming leg":

- Translational Eq. (8) is completely neglected, so only Eq. (9) is used for the simulation;
- The group of rotations $SO(3)$ in each joint is reduced to a single circle S^1, so that the three Euler angles (roll, pitch and yaw) in all four joints are replaced by single hinge-joint angles: $\varphi_i = (\varphi_1, \varphi_2, \varphi_3, \varphi_4) = (\varphi_{\text{hip}}, \varphi_{\text{knee}}, \varphi_{\text{ankle}}, \varphi_{\text{toes}})$, with the muscular torques acting in them: $T_i = (T_1, T_2, T_3, T_4) = (T_{\text{hip}}, T_{\text{knee}}, T_{\text{ankle}}, T_{\text{toes}})$;
- Both fluid-coupling terms ($\varepsilon^j_{ik} L_{\omega^j} \omega^k, \varepsilon^j_{ik} L_{v^j} v^k$) are neglected.
- All anthropometric measures (i.e., segment lengths, masses and inertia moments are normalized to 1.)
- The result of this simplification is the "robotic swimming leg," resembling a four-segment planar manipulator (see Vukobratovic and Potkonjak, 1982).

The following four equations of motion (with primes denoting time derivatives) are derived from this highly simplified Kirchhoff–Lagrangian dynamics model and numerically simulated using the standard Runge-Kutta 4 integrator (see Fig. 1):

Hip $\left(\boldsymbol{\varphi_{\text{hip}}}, \boldsymbol{T_{\text{hip}}}\right)$**-equation** $3\sin(\varphi_1(t) - \varphi_2(t))((\varphi_2)'(t))^2 + 2\sin(\varphi_1(t) - \varphi_3(t))((\varphi_3)'(t))^2 + \sin(\varphi_1(t) - \varphi_4(t))((\varphi_4)'(t))^2 + 4\cos(\varphi_1(t)) + 4(\varphi_1)''(t) + 3\cos(\varphi_1(t) - \varphi_2(t))(\varphi_2)''(t) + 2\cos(\varphi_1(t) - \varphi_3(t))(\varphi_3)''(t) + \cos(\varphi_1(t) - \varphi_4(t))(\varphi_4)''(t) = T_1(t)$,

Knee $(\boldsymbol{\varphi_{\text{knee}}}, \boldsymbol{T_{\text{knee}}})$**-equation** $2\sin(\varphi_2(t) - \varphi_3(t))((\varphi_3)'(t))^2 + \sin(\varphi_2(t) - \varphi_4(t))((\varphi_4)'(t))^2 + 3\cos(\varphi_2(t)) + 3\cos(\varphi_1(t) - \varphi_2(t))(\varphi_1)''(t) + 3(\varphi_2)''(t) + 2\cos(\varphi_2(t) - \varphi_3(t))(\varphi_3)''(t) + \cos(\varphi_2(t) - \varphi_4(t))(\varphi_4)''(t) = 3\sin(\varphi_1(t) - \varphi_2(t))((\varphi_1)'(t))^2 + T_2(t)$,

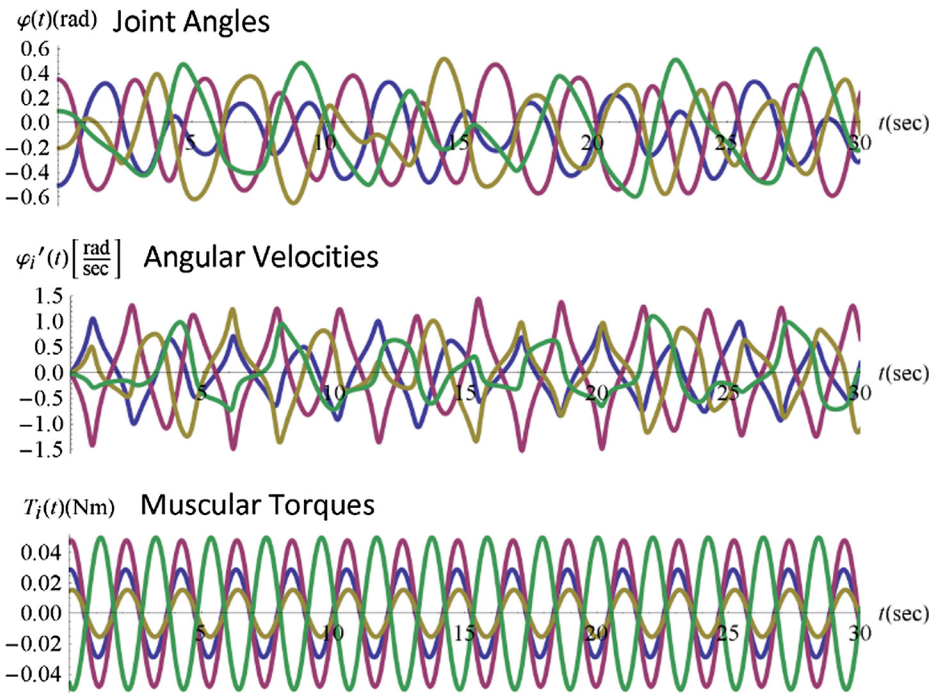

Fig. 1. A simplified (30 s) simulation of a robotic swimming leg. All anthropometric quantities of leg-segments (lengths, masses and inertia moments) are normalized to 1. Harmonic driving torques are given amplitudes of 0.1 Nm ± 0.5 (random), constant frequencies of and time delays of 0.1 s between the ith and i + 1st segments, to create the wavy propulsion. Joint angles are measured from the horizontal. The simulation shows coherent oscillations in all four joints similar to those induced by additive white noise (Burkett et al., 2001), which can serve as a natural synergetic model of musculoskeletal multistability (Assassi and Magnenat-Thalmann, 2014) in the leg-propulsion system.

Ankle $(\boldsymbol{\varphi}_{\mathbf{ankle}}, \boldsymbol{T}_{\mathbf{ankle}})$**-equation** $2\sin(\varphi_1(t)-\varphi_3(t))((\varphi_1)'(t))^2+2\sin(\varphi_2(t)-\varphi_3(t))((\varphi_2)'(t))^2=\sin(\varphi_3(t)-\varphi_4(t))((\varphi_4)'(t))^2+2(\cos(\varphi_3(t))+\cos(\varphi_1(t)-\varphi_3(t))(\varphi_1)''(t)+\cos(\varphi_2(t)-\varphi_3(t))(\varphi_2)''(t)+(\varphi_3)''(t))+\cos(\varphi_3(t)-\varphi_4(t))(\varphi_4)''(t)+T_3(t)$,

Toes $(\boldsymbol{\varphi}_{\mathbf{toes}}, \boldsymbol{T}_{\mathbf{toes}})$**-equation** $\cos(\varphi_4(t))+\cos(\varphi_1(t)-\varphi_4(t))(\varphi_1)''(t)+\cos(\varphi_2(t)-\varphi_4(t))(\varphi_2)''(t)+\cos(\varphi_3(t)-\varphi_4(t))(\varphi_3)''(t)+(\varphi_4)''(t)=\sin(\varphi_1(t)-\varphi_4(t))((\varphi_1)'(t))^2+\sin(\varphi_2(t)-\varphi_4(t))((\varphi_2)'(t))^2+\sin(\varphi_3(t)-\varphi_4(t))((\varphi_3)'(t))^2+T_4(t)$.

4. Discussion and conclusion

We have developed a dynamical model of the legs motion through the water medium in freestyle and backstroke swimming, proposed as a low-to-moderate intensity rehabilitation exercise after hip and knee surgery. However, both the proposed model and the associated rehabilitation exercise can be also applied to swimming rehabilitation of patients with amputations. For a review of biomechanical models in the study of lower limb amputee kinematics, see (Kent and Franklyn-Miller, 2011) and the references therein. Biomechanical studies of amputations can be anatomically classified to: (i) prosthetic knee joint, like (Andrysek and Chau, 2007), where the energy transfer mechanisms of a swing phase controlled knee joint were evaluated, and (Burkett et al., 2001), where the trans-femoral prosthetic alignment was optimized for running, by lowering the knee joint, and (ii) foot/ankle prosthetics, like (Long et al., 2010), where sources of variability in multi-center assessment of segmental foot kinematics were analyzed, and (Burkett et al., 2001), where trans-femoral prosthetic alignment for running was optimized by lowering the knee joint.

On the validation side, the simulated joint angles and muscular torques presented in Fig. 1 are similar to the average flexion/extension joint angles and total torques of the leg joints over the gait cycle in the lower extremity exoskeleton presented in Dollar and Herr (2007) (Fig. 3) and to some extent to the speed-matched mean patterns of sagittal plane hip, knee and ankle joint angles over the gait cycle presented in Su et al. (2008) (Figs. 1–3).

Finally, while the "robotic swimming leg" is recommended both as a rehabilitation exercise and as a proof of the general concept, we emphasize that the full biomechanical simulation of a human swimming leg would implement the full tensor Kirchhoff–Lagrangian equations (8)–(9).

Declaration of Competing Interest

The authors declare that they have no conflict of interest.

Ethical approval

This article does not contain any studies with human participants or animals performed by any of the authors.

References

Andrysek, J., Chau, G., 2007. An electromechanical swing-phase-controlled prosthetic knee joint for conversion of physiological energy to electrical energy: feasibility study. IEEE Trans. Biomed. Eng. 54 (12), 2276–2283.
Ardestani, M.M., ZhenXian, C., Noori-Dokht, H., Moazen, M., Jin, Z., 2019. Computational analysis of knee joint stability following total knee arthroplasty. J. Biomech. 86, 17–26.
Assassi, L., Magnenat-Thalmann, N., 2014. A biomechanical approach for dynamic hip joint analysis. In: Magnenat-Thalmann, N., Ratib, O., Choi, H. (Eds.), 3D Multiscale Physiological Human. Springer, London.
Burkett, B., Smeathers, J., Barker, T., 2001. Optimising the trans-femoral prosthetic alignment for running, by lowering the knee joint. Prosthet. Orthot. Int. 25 (3), 210–219.
Dollar, A.M., Herr, H., 2007. Lower extremity exoskeletons and active orthoses: challenges and state-of-the-art. IEEE Trans. Rob. 24 (1), 144–158.
Duval, N., St-Onge, N., 1997. Passive and dynamic stability of the knee joint. In: Yahia, L'H. (Ed.), Chapter in Ligaments and Ligamentoplasties. Springer, Berlin, pp. 19–37.

Gallo, J., Goodman, S., Lostak, J., Janout, 2012. Advantages and disadvantages of ceramic on ceramic total hip arthroplasty: A review. Biomedical papers of the Medical Faculty of the University Palacký, Olomouc, Czechoslovakia. 156, 204–212.
Gojkovic, Z., 2015. Implantation of the knee joint endoprosthesis. Medical Survay, Novi Sad, LXVIII 11–12, 367–369.
Gojkovic, Z., Ivancevic, T., 2016. Control of the extension-flexion cycle of human knees during bicycle riding by a synergy of solitary muscular excitations and contractions. Nonlinear Dyn. 90 (3), 2047–2056.
Gojkovic, Z., Ivancevic, T., Jovanovic, B., 2017. A two-phase computational biomechanics model for successful rehabilitation after hip and knee surgery. Nonlinear Dyn. 86 (3), 2071–2080.
Gourgoulis, V., Aggeloussis, N., Vezos, N., Kasimatis, P., 2008. Estimation of hand forces and propelling efficiency during front crawl swimming with hand paddles. J. Biomech. 41, 208–215.
Ivancevic, V.G., 2009. New mechanics of generic musculo-skeletal injury. Biophys. Rev. Lett. 4 (3), 273–287.
Ivancevic, T., 2010a. Jet methods in time-dependent lagrangian biomechanics. Cent. Eur. J. Phys. 8 (5).
Ivancevic, T., 2010b. Jet-Ricci geometry of time-dependent human biomechanics. Int. J. Biomathematics 3 (1), 1–13.
Ivancevic, V., Ivancevic, T., 2006. Geometrical Dynamics of Complex Systems. Springer, Dordrecht.
Ivancevic, V., Ivancevic, T., 2006. Human-Like Biomechanics. Springer, Dordrecht.
Ivancevic, V., Ivancevic, T., 2008. Human versus humanoid biodynamics. Int. J. Humanoid Rob. 5 (4), 699–713.
Ivancevic, V., Ivancevic, T., 2012. New Trends in Control Theory. World Scientific, Singapore.
Ivancevic, T., Lukman, L., Gojkovic, Z., Greenberg, R., Greenberg, H., Jovanovic, B., Lukman, A., 2017. The Evolved Athlete: A Guide for Elite Sport Enhancement. Springer, Berlin.
Ivancevic, T., Jovanovic, B., Gojkovic, Z., 2019. Comprehensive review of the universal jolt mechanism theory for musculoskeletal injuries. In: Reconstructions, Ligament (Ed.), Chap. 12 in L'Hocine Yahia. World Scientific, Singapore.
Kent, J., Franklyn-Miller, A., 2011. Biomechanical models in the study of lower limb amputee kinematics: a review. Prosthet. Orthot. Int. 35 (2), 124–139.
Konopka, J.F., Lee, Y., Su, E.P., McLawhorn, A.S., 2018. Quality-adjusted life years after hip and knee arthroplasty. J. Bone Joint Surg. 3 (3), e0007.
Lamb, H., 1932. Hydrodynamics. Dover, New York.
Leonard, N.E., 1997. Stability of a bottom-heavy underwater vehicle. Automatica 33 (3), 331–346.
Long, J.T., Eastwood, D.C., Graf, A.R., Smith, P.A., Harris, G.F., 2010. Repeatability and sources of variability in multi-center assessment of segmental foot kinematics in normal adults. Gait Posture 31 (1), 32–36.
Michele, A.A., 1962. Iliopsoas; development of anomalies in man. Thomas Pub, Springfield, Ill.
O'Connor, J.D., Rutherford, M., Bennet, D., Hii, J.C., Beverland, D.E., Dunne, N.J., Lennon, A.B., 1999. Long-term hip loading in unilateral total hip replacement patients is no different between limbs or compared to healthy controls at similar walking speeds. J. Biomech. 80, 8–15. 2018.
Prins, J., Cutner, D., 1999. Aquatic therapy in the rehabilitation of athletic injuries. Clin. Sports Med. 18 (2), 447–461.
Rolfson, O., Bohm, E., Franklin, P., et al., 2016. Patient-reported outcome measures in arthroplasty registries. Acta Orthopaedica 87, 9–23.
Sjolander, P., Johansson, H., 1997. Sensory endings in ligaments: response properties and effects on proprioception and motor control. In: Yahia, L'H. (Ed.), Chapter in Ligaments and Ligamentoplasties. Springer, pp. 39–83.
St-Onge, N., Duval, N., Yahia, L'H., Feldman, A., 2004. Interjoint coordination in lower limbs in patients with a rupture of the anterior cruciate ligament of the knee joint. Knee Surg. Sports Traumatol. Arthrosc. 12 (3), 203–216.
Su, P.F., Gard, S.A., Lipschutz, R.D., Kuiken, T.A., 2008. Differences in gait characteristics between persons with bilateral transtibial amputations, due to peripheral vascular disease and trauma, and able-bodied ambulators. Arch. Phys. Med. Rehabil. 89 (7), 1386–1394.
Takagi, H., Nakashima, M., Sato, Y., Kazuo, M., Sanders, R.H., 2016. Numerical and experimental investigations of human swimming motions. J. Sports Sci. 34 (16), 1564–1580.
Vaz, J.R., Olstad, B.H., Cabri, J., Kjendlie, P.-L., Pezarat-Correia, P., Hug, F., 2016. Muscle coordination during breaststroke swimming: comparison between elite swimmers and beginners. J. Sports Sci. 34 (20), 1941–1948.
Veiga, S., Roig, A., Gómez-Ruano, M.A., 2016. Do faster swimmers spend longer underwater than slower swimmers at World Championships? Eur. J. Sport Sci. 16 (8), 919–926.
Vukobratovic, M., Potkonjak, V., 1982. Scientific Fundamentals of Robotics. Dynamics of Manipulation Robots: Theory and Application, Vol. 1. Springer, Berlin.
Yahia, L'H. (Ed.), 1997. Ligaments and Ligamentoplasties. Springer, New York.
Yahia, L'H., 2015. Shape Memory Polymers for Biomedical Applications. Elsevier.
Yahia, L.H., Rhalmi, S., Newman, N., Isler, M., 1992. Sensory innervation of human thoracolumbar fascia: an immunohistochemical study. Acta Orthop. Scand. 63 (2), 195–197.
Yahia, L.H., Pigeon, P., DesRosiers, E.A., 1993. Viscoelastic properties of the human lumbodorsal fascia. J. Biomed. Eng. 15 (5), 425–429.
Zaidi, H., Taiar, R., Fohanno, S., Polidori, G., 2008. Analysis of the effect of swimmer's head position on swimming performance using computational fluid dynamics. J. Biomech. 41, 1350–1358.